

Trends of atmospheric circulation during singular hot days in Europe

Aglaé Jézéquel, Julien Cattiaux, Philippe Naveau, Sabine Radanovics, Aurélien Ribes, Robert Vautard, Mathieu Vrac, Pascal Yiou

E-mail: aglae.jezequel@lsce.ipsl.fr

Abstract. The influence of climate change on mid-latitudes atmospheric circulation is still very uncertain. Because of the large internal variability, it is difficult to extract any significant signal regarding the evolution of the circulation. Here we propose a methodology to calculate dynamical trends tailored to the circulation of specific days by computing the evolution of the distances between the circulation of the day of interest and the other days of the time series. We compute these dynamical trends for two case studies of the hottest days recorded in two different European regions (corresponding to the heatwaves of summer 2003 and 2010). We use the NCEP reanalysis dataset, an ensemble of CMIP5 models, and a large ensemble of a single model (CESM), in order to account for different sources of uncertainty. While we find a positive trend for most models for 2003, we cannot conclude for 2010 since the models disagree on the trend estimates.

Submitted to: *ERL*

1. Introduction

Extreme event attribution [Stott et al., 2016] aims at evaluating how the properties of a specific extreme climate event have been affected by anthropogenic forcings. Climate change may play a role on either — or both — the dynamics and the thermodynamics explaining the event. The influence of climate change on the thermodynamics of European heatwaves has been largely studied and proven for both specific events (e.g. Stott et al. [2004], Christidis et al. [2015], Russo et al. [2015]) and types of events (e.g. heatwaves in Russo et al. [2014]). The evolution of the dynamics related to heatwaves is still a debated subject. Most of the studies evaluating whether climate change has an influence on the atmospheric circulation in mid-latitudes are not event-specific.

The atmospheric dynamics in the Northern Hemisphere mid-latitudes are driven by the latitudinal temperature gradient. This gradient could be modified by climate

change through two processes: the surface Arctic amplification (AA) and the upper-tropospheric tropical warming (Peings et al. [2017]). The evolution of those two factors is still very uncertain, with a wide range of responses across climate models (Zappa and Shepherd [2017]), and even across different members of a single model ensemble due to internal variability (Deser et al. [2016], Peings et al. [2017]).

Over Europe, the link between long-lasting anticyclonic circulation, called blockings (e.g. Ruti et al. [2014]), and high summer temperatures has been established (e.g. Jézéquel et al. [2017a], Cassou et al. [2005], Yiou and Nogaj [2004]). Francis and Vavrus [2012] detected the emergence of a significant increase in the persistence of blockings over the recent years using a reanalysis dataset. They explain this emergence by a mechanism based on the AA. Coumou et al. [2015] found similar results focusing on summer and using satellite data. However, Barnes [2013] argue that the results of Francis and Vavrus [2012] depend on the methodology they used and could be subject to ambiguous interpretations. Cattiaux et al. [2016] used global climate models (GCM) to extend the search of trends to the twenty-first century. They found no evidence of an increase of persistence of blockings. Those studies evaluate the evolution of the circulation on large scales, on either the whole Northern Hemisphere or the North Atlantic region. In this paper, we are interested in capturing trends related to specific heatwave events, and we hence focus on a more regional scale.

Ruti et al. [2014] calculated summer trends of the blocking index defined by Tibaldi and Molteni [1990] over the Euro-Russian region using a reanalysis dataset and an atmospheric-only model for the 20th century. They found an increase in the duration of blocking episodes for the second part of the century, which they attribute to climate change, using different forcings as inputs of their model. However, the 20th century might not be long enough to evaluate trends on blockings. Indeed, using a large ensemble from a single model representing internal variability, Peings et al. [2017] found a decrease in the blocking index over the 1920–2100 period for the North Atlantic region, which includes Ruti et al.’s Euro-Russian region. Those differences could be related to an inconsistency between different models or to different evaluations of the internal variability. We hence used a set of different models and a large ensemble to account for both.

Trenberth et al. [2015] argued that due to the large internal variability of dynamical processes, it is best to focus only on thermodynamical processes for a fixed dynamical state in order to extract the signal related to climate change. A few attribution studies that condition the signal to the circulation follow this approach to extract thermodynamical signals hidden in a large internal variability [e.g., Cattiaux et al., 2010, Meredith et al., 2015]. However, this does not allow to calculate the complete influence of climate change on the events of interest [Otto et al., 2016]. Shepherd [2016] highlighted that it is possible to study the dynamic and thermodynamic contributions separately. Few papers have studied the influence of climate change on the dynamics applied to a singular

event [Vautard et al., 2016, Yiou et al., 2017]. Jézéquel et al. [2017b] found no detectable influence of climate change on the occurrence of the circulation leading to the extremely warm December month of 2015 in France. In this paper, we extend the ideas introduced by Jézéquel et al. [2017b] in an effort to focus on the evolution of the dynamics related to specific events. Our goal is to propose a systematic way to detect this evolution for any given day of interest and for any given region. We used the distances between 2-dimensional fields of geopotential height at 500hPa (Z500) as a metric to capture the similarity of local patterns of circulation related to specific days. Our case studies are record hot days, as they matter the most in terms of impacts [Seneviratne et al., 2016]. We did not study here the evolution of thermodynamical processes related to heatwaves in Europe (e.g. soil moisture, as explained in Seneviratne et al. [2010]).

We seek to detect changes in the occurrence of circulation patterns related to specific hot days. We leave the attribution of those changes to further studies. We first present a methodology to estimate trends of the circulation for a given daily event. We then apply this methodology to two case studies: the 2003 heatwave in Western Europe and the 2010 heatwave in Russia. We finally discuss those findings and potential larger applications of our methodology to other types of events.

2. Data and Methods

2.1. Datasets

In this study, we assume that the geopotential height at 500hPa (Z500) is a proxy for the extra-tropical atmospheric circulation. We focus on the summer season (June-July-August: JJA). We use daily averages of Z500 from three datasets over two European subregions: [20W–20E; 40N–60N], called Western Europe (WE) hereafter and [10E–68E; 45N–70N], called Russia (RU) hereafter.

The first dataset is the National Centers for Environmental Prediction/National Center for Atmospheric Research, NCEP/NCAR, reanalysis I dataset [Kalnay et al., 1996] between 1950 and 2016, called NCEP hereafter. Its horizontal resolution is 2.5 degree by 2.5 degree. This dataset, called \mathcal{A}_1 hereafter, allows us to assess whether dynamical trends are detectable in a short dataset, which is as close as possible to the observations.

The second dataset is an ensemble of 18 models from the fifth Coupled Model Inter-comparison Project (CMIP5) (Taylor et al. [2012], a table with all the models references and resolutions is available in the supplementary material) with easily accessible Z500 on the IPSL (Institut Pierre Simon Laplace) cluster. They cover the 1950–2100 period, with a historical simulation from 1950 to 2005 and RCP4.5 and RCP8.5 scenarios from

2006 to 2100. This multi-model dataset is named \mathcal{A}_2 .

The third dataset consists of 30 runs of the Community Earth System Model large ensemble (CESM-LENS) [Kay et al., 2015]. The model horizontal resolution is 1 degree by 1 degree. It covers the 1950 – 2100 period with a historical simulation for the 1950 to 2005 period and the RCP8.5 scenario from 2006 to 2100. This ensemble dataset is named \mathcal{A}_3 .

The rationale for using those three types of data is that this allows to compare reanalysis data with a single model ensemble (CESM-LENS) that reflects the internal variability of a climate model and a multi-model ensemble (CMIP5) that reflects the uncertainty due to the model formulation. This allows in turn to estimate different components of the uncertainty (see Section 2.3).

Historical runs over 1950–2005 are merged with RCP8.5 runs over the 2006–2016 period to allow the comparison with reanalysis data over the whole 1950–2016 period. The choice of RCP8.5 is (1) coherent with observations and (2) the only scenario available for CESM-LENS.

In this article, we focus on very hot days, which are related to anticyclonic blocking situations. We are therefore interested in finding close Z500 patterns to those types of circulation. The Z500 is however related to the lower-tropospheric temperature, so that a global surface warming results in a generalized Z500 increase. In order to focus on the dynamical signal and ensure that our method would not interpret a uniform Z500 rise as a change in circulation, we choose to remove this background thermal effect (contrarily to Horton et al. [2015]). This is done by subtracting a spatially uniform trend, calculated on the mean seasonal (JJA) spatial average on the region of interest, using a cubic smoothing spline in time (similarly to Jézéquel et al. [2017a]). By subtracting a uniform field, we do not alter the horizontal gradients of Z500 that depict the circulation. An alternative to using Z500 would have been to use SLP but in summer, the SLP field is affected by a heat low effect that blurs the dynamical signal (Jézéquel et al. [2017a]).

2.2. Dynamical trend estimation

Our goal is to determine whether a given circulation pattern has become more or less frequent during a given period. We consider a Z500 reference pattern Z^d belonging to the dataset \mathcal{A}_1 that occurs on a day d . For all the days d' in the dataset \mathcal{A}_k , we compute the set of Euclidean distances between $Z^{d'} \in \mathcal{A}_k$ and the reference $Z^d \in \mathcal{A}_1$. For the reanalysis dataset, we exclude the days within the same year as the event of interest. We determine the x th quantile q_x of those distances for each separate dataset \mathcal{A}_k (the value of q_x can hence differ depending on the dataset). The value of x can be

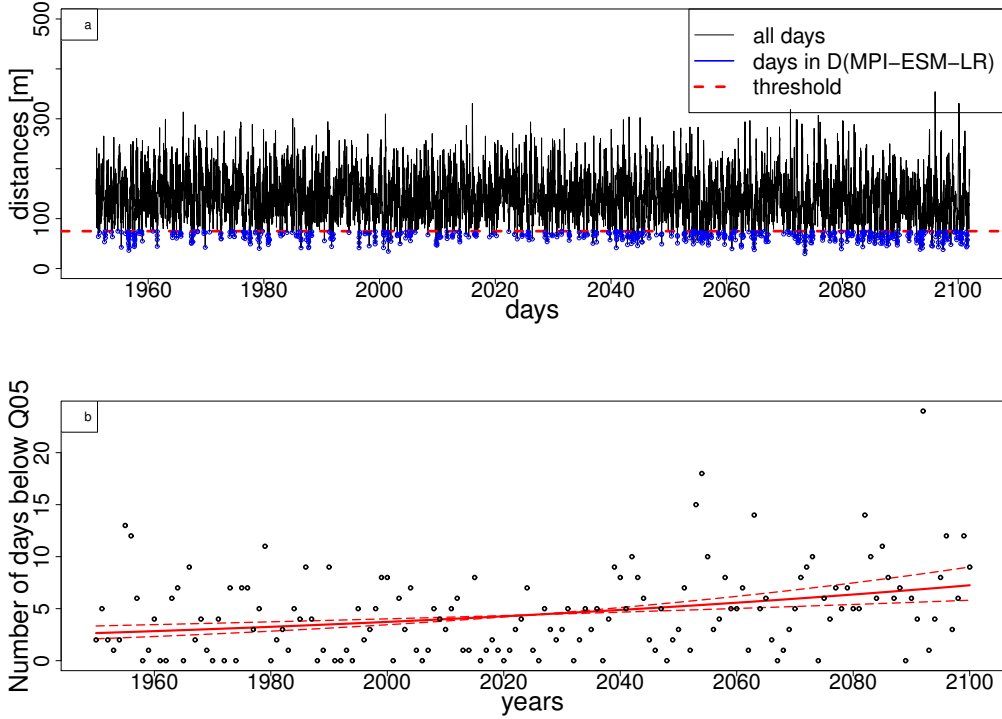


Figure 1: Example for August 13th 2003 over the region $[20W-20E;40N-60N]$ with the MPI-ESM-LR model and the RCP8.5 scenario. a) time series of daily Euclidean distances between $Z_{d'}$ and Z_d . The 5th percentile is represented by the red dotted lines. The blue points are the days in $D(Z_d)$. b) Evolution of the number of days belonging to $D(Z^d)$, N_y . The black dots represent N_y . The red straight line is the modeled $E(N_y)$ using the glm, the dotted lines represent the confidence interval.

chosen heuristically, e.g. the 5th quantile. From Z^d and q_x we define the class of days or patterns $D(Z^d)$ in the ensemble \mathcal{A}_k that are similar to Z^d :

$$D(Z^d) = \{d' \in \mathcal{A}_k, \text{dist}(Z^{d'}, Z^d) \leq q_x\}. \quad (1)$$

The class $D(Z^d)$ is shown for August 13th 2003 over the WE region for one model of \mathcal{A}_2 (MPI-ESM-MR) in Figure 1a (blue dots).

For each year y in \mathcal{A}_k , we count the number N_y of days in $D(Z^d)$ in order to study potential trends in N_y . This requires to properly model the evolution of this variable. The first step is to find a suitable distribution to describe it. The variable N_y is discrete and bounded. N_y can only take integer values between 0 and $N_{tot} = 92$ (the number of days in JJA). We display the evolution of N_y with time in Figure 1b for one model. As $\text{Var}(N_y)$ is 2.0 to 15.2 times larger than the expected value $E(N_y)$, we conclude that the distribution of N_y is systematically overdispersed with respect to a Poisson or to a

binomial distribution (with parameter p), for which the variances would be respectively equal to $E(N_y)$ and $(1 - p)E(N_y)$.

From a physical point of view, this overdispersion is a consequence of the temporal autocorrelation of Z500 related to the persistence of atmospheric circulation. This autocorrelation is particularly strong in the case of hot days, since they are related to long-lasting blocking situations. The odds of having another day in $D(Z^d)$ within a given year increase with the number of days already in $D(Z^d)$ within the summer. We chose to model the distribution as a beta-binomial distribution, which fits well bounded discrete distributions that are overdispersed, so that:

$$P(N_y = k) = \binom{N_{tot}}{k} \frac{B(k + \alpha, N_{tot} - k + \beta)}{B(\alpha, \beta)} \quad (2)$$

where B is the beta function (Whittaker and Watson [1996]), and α and β parameters which allow to account for a possible overdispersion.

The second step is to find a statistical model to describe the evolution of N_y with time. Therefore we used a generalized linear model (glm, see Eq. (4)) to determine the temporal trend of N_y (Nelder and Wedderburn [1972]). The glm is a generalization of the linear regression through the use of a link function g allowing the transformed mean to vary as a function of predictors. We transform the mean as $g(E(N_y/N_{tot}))$ where

$$g(u) = \log(u/(1 - u)), \quad (3)$$

with $u \in [0, 1]$ and $E(\cdot)$ is the expected value. g is called the *logit* link function.

We used the R package VGAM [Yee, 2010], which includes the function `vglm` that fits a glm to beta-binomial distributions [Prentice, 1986].

For a year y in \mathcal{A}_k , we assume that:

$$g(E(N_y/N_{tot})) = \alpha_N + \beta_N y, \quad (4)$$

where α_N and β_N are the regression coefficients.

The interpretation of regression coefficients is not straightforward, because the glm uses the logit link function, which produces a non-linear regression. We therefore present the results using fitted values of $E(N_y)$. We used the inverse link function $E(N_y) = N_{tot} \times g^{-1}(\alpha_N + \beta_N y)$ and the regression coefficients to obtain the fitted values of $E(N_y)$ for year y , which gives the red line in Figure 1b. We then calculated the difference between the fitted values of $E(N_y)$ between the end and the beginning of the time series, in order to analyze the evolution of $E(N_y)$. We denote that the regression

is not too far from a linear regression (see Fig 1b).

This regression is a way to determine whether the days similar to Z^d get more (or less) likely with time. However, it does not discriminate whether any change detected is related to the fact that days close to Z^d happen more regularly every summer, or if they are more numerous within a given event. Decomposing those two parts of the signal is beyond the scope of the present article.

2.3. Uncertainties

In order to derive a confidence interval on the estimated trend, we first calculated a confidence region for β_N – this is done assuming that $\hat{\beta}_N$ follows a Gaussian distribution. This confidence interval on β_N can then be translated into a confidence interval on the average number of days belonging to $D(Z^d)$, by calculating the fitted values of $E(N_y)$ corresponding to the upper (resp. lower) bound of β_N . We consider that the change is significant if the confidence interval on β_N does not include 0.

Besides the statistical uncertainty, the two ensemble datasets allow to evaluate the uncertainty due to internal variability in the case of CESM-LENS \mathcal{A}_3 and the multi-model uncertainty in the case of the CMIP5 ensemble \mathcal{A}_2 . The internal variability should be included in the multi-model variability.

The comparison of those three sources of uncertainties allows us to detect whether the circulation undergoes a significant evolution. It also weighs the sources of uncertainties and assesses the confidence in the methodology. We cannot attribute any detected evolution to climate change with this methodology, as we do not compare our results to those which could be obtained in a world without climate change.

3. Two case studies

We chose two epitomes of heatwaves of the 21st century, largely studied in the literature to apply our method: summer 2003 (e.g. Beniston [2004], Fischer et al. [2007], Stéfanon et al. [2012]) in the WE region and summer 2010 (e.g. Dole et al. [2011], Rahmstorf and Coumou [2011], Trenberth and Fasullo [2012], Otto et al. [2012], Hauser et al. [2016]) in the RU region. The thermodynamical component of climate change has been identified by those authors, but the dynamical contribution has not been as emphasized. We used those two cases as examples to apply our methodology to detect circulation trends.

The hottest day of the NCEP reanalyses in the WE region was recorded on August 13th 2003, and the hottest day in the RU region was recorded on August 7th 2010 (for

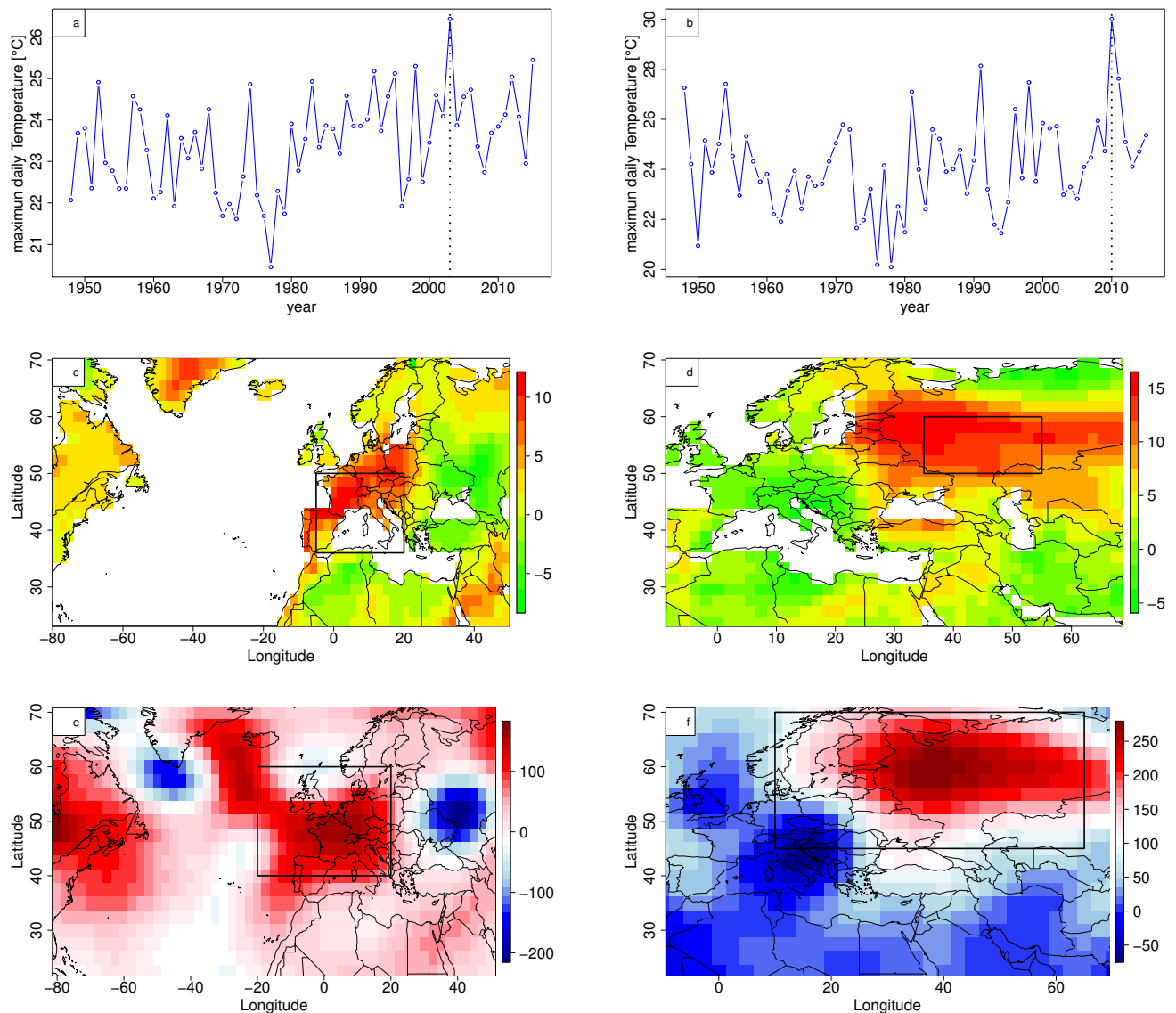


Figure 2: Two case studies: August 13th 2003 and August 7th 2010 using the NCEP dataset. a (respectively b) Time series of the yearly hottest summer day in the black boxes of figure 1c (respectively 1d) of 2003 (respectively 2010). c (and d): temperature anomaly of August 13th 2003 (August 7th 2010). e (and f): detrended Z500 anomaly of August 13th 2003 (August 7th 2010).

both absolute value and summer seasonal anomalies), as shown in figures 3(a) and 3(b). Figures 2c and 2d display the temperature anomalies for those days. The rectangles on those maps delimit the WE and RU regions (as defined in Jézéquel et al. [2017a] and Barriopedro et al. [2011]). Figures 2e and 2f show the corresponding daily maps of Z500 anomalies. The rectangles on those maps are regions selected based on the position of the anticyclonic anomaly (as in Jézéquel et al. [2017a]) to calculate the distances between the circulation of the day of interest and the circulation of the other summer

days in the times series.

Figure 3 displays the results of equation (2) with the 5th percentile. For the historical period, we get similar results for both 2003 and 2010. We detect no significant trend in NCEP for both events. In the case of August 13th 2003, CanESM2 and 3 runs of CESM-LENS have significant positive trends, and one run of CESM-LENS has a significant negative trend when only taking into account years from 1950 to 2016. The other models and runs display no significant trend. The bigger uncertainty comes from the internal variability assessed with CESM-LENS. This means that we cannot judge the quality of a model with respect to the simulation of dynamical trends by comparing it to the NCEP reanalysis, which is just one realization of what could have happened for the same background state of the climate. The multi-model uncertainty is smaller than the internal variability. This could mean that 18 CMIP5 models are not enough to capture internal variability. Alternatively, CESM-LENS could overestimate the internal variability. In the case of August 7th 2010, no model detects either a positive or a negative significant trend on the historical period. The statistical uncertainty is larger than for 2003. The multi-model uncertainty equals the internal variability. Using only reanalyses or historical runs of 67 years is not sufficient to detect any significant signal. A potential signal does not emerge from internal variability for neither of the two regions and both types of circulation. This is coherent with the findings of Deser et al. [2016] who have shown that SLP trends over the North Atlantic region have different signs for different runs of CESM-LENS even over 50 years, although the focus of their study was the winter season. We get past the internal variability using 151 years (from 1950 to 2100) and RCP scenarios.

For the longer periods, the results differ between 2003 and 2010. For the former, 7 models detect a significant positive signal, 8 models detect a non significant positive signal, and 3 models detect a non significant negative signal for RCP4.5. For RCP 8.5, 10 models detect a significant positive signal, 7 models a non significant positive signal and 1 model a non significant negative signal. Out of the 30 runs of CESM-LENS, 29 detect significant positive difference between 1950 and 2100 and the last one detects a non significant positive difference. Although the response differs from one model to another, there seems to be an agreement on a positive difference of approximately 5 days in 151 years. With the choice of the 5th percentile to define $D(Z^d)$, the mean number of days in $D(Z^d)$ for each summer is approximately 4 days. Therefore a difference of 5 days is not negligible. The models do not agree as much for 2010 as for 2003. For RCP4.5, we find 2 models with a significant positive trend, 10 models with non significant positive trends and 6 models with non significant negative trends. For RCP8.5, we find 4 models with significantly positive trends, 3 models with significantly negative trends, 5 models non significant positive trends, and 6 models with non significant negative trends. Out of the 30 runs of CESM-LENS, 27 yield a significantly positive trend and 3 have non significant positive trends. The models hence strongly disagree, which questions the

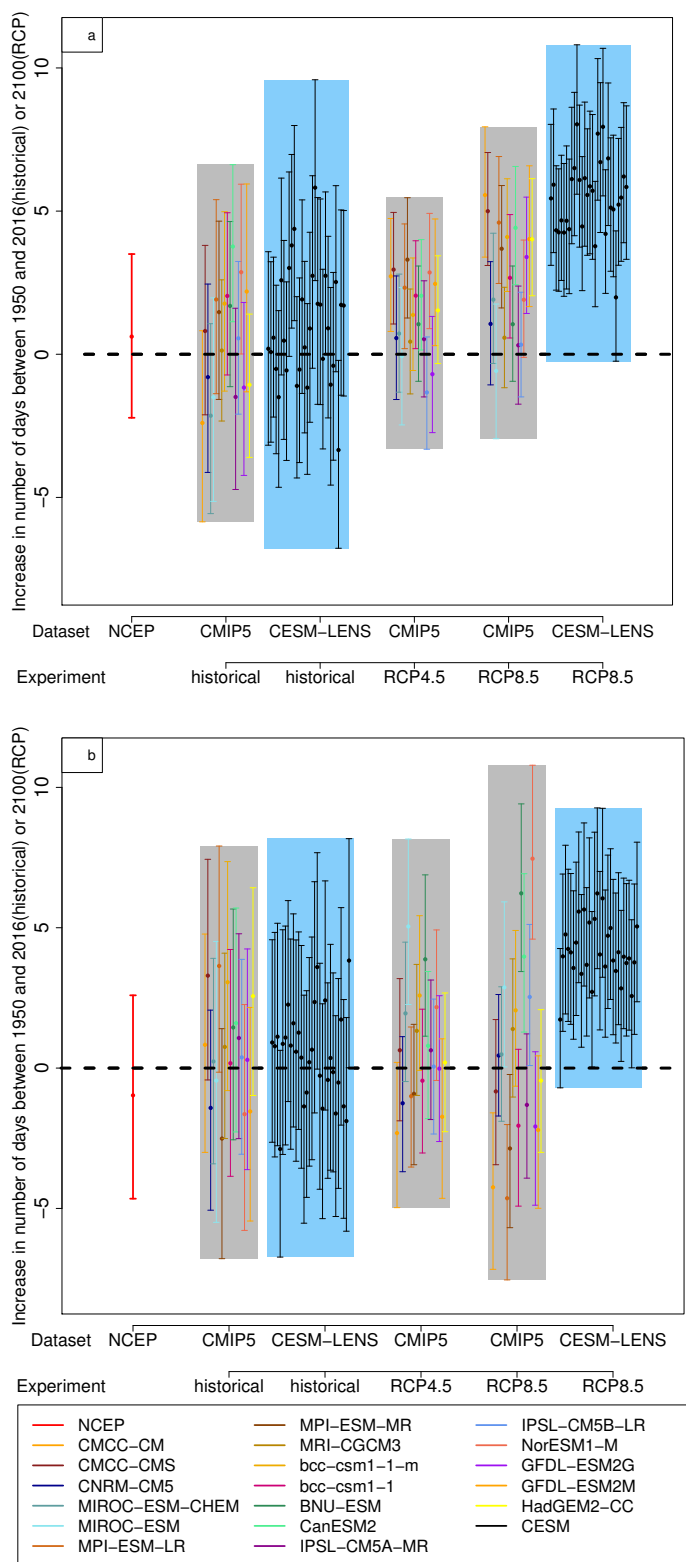


Figure 3: Dynamical trends. Panels a and b display the modeled difference between the average number of days N_{end} and $N_{beginning}$ belonging to $D(Z^d)$ for NCEP (in red), CMIP5 (bars in gray shaded areas) and CESM (bars in blue shaded), for the historical, RCP4.5 and RCP8.5 experiments. Panel a is for August 13th 2003. Panel b is for August 7th 2010.

robustness of trends found in studies where only one model is used.

4. Discussion

Our methodology gives different results for 2003 and 2010. While we find a positive signal with most models for 2003, the models do not show coherence for 2010. This could be related to the physics associated with the two events. The fact that the results are reinforced between RCP4.5 and RCP8.5 is an argument in favor of attributing the significant changes in the weather pattern of one central day of the 2003 heat wave to climate change. If the models that detect significant positive trends are to be believed, this could mean longer and more frequent heatwaves similar to 2003 in Western Europe, without even taking into account the thermodynamical effect of climate change on temperature, which has been largely proven in the literature (e.g. Meehl and Tebaldi [2004], Bador et al. [2017]). Peings et al. [2017] find a decrease in the one-dimensional blocking index as defined by Tibaldi and Molteni [1990], which would indicate a lesser importance of the dynamics in the years to come, even though they use the same CESM-LENS dataset as us. The difference between both results shows how the focus on a specific dynamical event through the use of a two-dimensional Z500 field can give a different information than a general outlook on circulations leading to heatwaves. Even in the case where we detect a significant dynamical trend, it is noteworthy that dynamical trends are less important than thermodynamical trends.

All the Z500 fields were detrended to remove from Z500 the thermodynamical influence of climate change. However, the shape of the modeled Z500 distribution can differ from the observed one. We tested 4 types of normalization: no normalization, a simple normalization (division by the standard deviation) on every grid-point, a simple normalization on the mean of the Z500 field and a quantile-mapping (e.g. Panofsky and Brier [1958], Déqué [2007], and Gudmundsson et al. [2012]). We normalized using the 1950-2005 period which is common between historical runs and NCEP. Although the normalization changes results for a few individual models (in particular for CNRM-CM5), it does not change the collective results of the ensemble of CMIP5 and CESM-LENS models (not shown here). Since the normalization does not fundamentally change our results, we use non normalized Z500 fields.

We also tested how the results change when we choose a different percentile to define $D(Z^d)$. We tested 4 percentiles: the 2th, the 5th, the 10th and the 25th percentiles. With the increase of the percentile we get more days on which to calculate trends. The differences detected between the 1950 and 2100 values of N_y monotonically increase with the percentile. The results get more significant (further from 0 and in some cases become significant) for higher percentiles. However, because we are interested in specific events, we keep the 5th percentile which we consider to be more relevant for this study.

- Winter 2010 in Europe: A cold extreme in a warming climate. *Geophysical Research Letters*, 37(20):1–6, 2010. ISSN 00948276. doi: 10.1029/2010GL044613.
- J. Cattiaux, Y. Peings, D. SaintMartin, N. TrouKechout, and S. J. Vavrus. Sinuosity of midlatitude atmospheric flow in a warming world. *Geophysical Research Letters*, 43(15):8259–8268, 2016.
- N. Christidis, G. S. Jones, and P. A. Stott. Dramatically increasing chance of extremely hot summers since the 2003 European heatwave. *Nature Clim. Change*, 5(1):46–50, jan 2015. ISSN 1758-678X. URL <http://dx.doi.org/10.1038/nclimate2468> <http://10.1038/nclimate2468> <http://www.nature.com/nclimate/journal/v5/n1/abs/nclimate2468.html#supplementary-infor>
- D. Coumou, J. Lehmann, and J. Beckmann. The weakening summer circulation in the Northern Hemisphere mid-latitudes. *Science*, 348(6232):324–327, 2015. ISSN 0036-8075. doi: 10.1126/science.1261768. URL <http://science.sciencemag.org/content/348/6232/324>.
- M. Déqué. Frequency of precipitation and temperature extremes over France in an anthropogenic scenario: Model results and statistical correction according to observed values. *Global and Planetary Change*, 57(1):16–26, 2007. ISSN 0921-8181. doi: <https://doi.org/10.1016/j.gloplacha.2006.11.030>. URL <http://www.sciencedirect.com/science/article/pii/S0921818106002748>.
- C. Deser, J. W. Hurrell, and A. S. Phillips. The role of the North Atlantic Oscillation in European climate projections. *Climate Dynamics*, 0(0):1–17, 2016. ISSN 14320894. doi: 10.1007/s00382-016-3502-z. URL "<http://dx.doi.org/10.1007/s00382-016-3502-z>."
- R. Dole, M. Hoerling, J. Perlwitz, J. Eischeid, P. Pegion, T. Zhang, X. W. Quan, T. Xu, and D. Murray. Was there a basis for anticipating the 2010 Russian heat wave? *Geophysical Research Letters*, 38(6):1–5, 2011. ISSN 00948276. doi: 10.1029/2010GL046582.
- E. M. Fischer, S. I. Seneviratne, P. L. Vidale, D. Luthi, and C. Schar. Soil moisture - Atmosphere interactions during the 2003 European summer heat wave. *Journal of Climate*, 20(20):5081–5099, 2007. doi: Doi 10.1175/Jcli4288.1. URL <Go to ISI>: [//000250105900004](http://000250105900004).
- J. A. Francis and S. J. Vavrus. Evidence linking Arctic amplification to extreme weather in mid-latitudes. 39(February):1–6, 2012. doi: 10.1029/2012GL051000.
- L. Gudmundsson, J. B. Bremnes, J. E. Haugen, and T. Engen-Skaugen. Downscaling RCM precipitation to the station scale using statistical transformations—a comparison of methods. *Hydrology and Earth System Sciences*, 16(9):3383–3390, 2012.
- M. Hauser, R. Orth, and S. I. Seneviratne. Role of soil moisture versus recent climate change for the 2010 heat wave in western Russia. 2016. doi: 10.1002/2016GL068036.Received.

- D. E. Horton, N. C. Johnson, D. Singh, D. L. Swain, B. Rajaratnam, and N. S. Diffenbaugh. Contribution of changes in atmospheric circulation patterns to extreme temperature trends. *Nature*, 522(7557):465–469, 2015. ISSN 0028-0836. doi: 10.1038/nature14550. URL <http://www.nature.com/doifinder/10.1038/nature14550>.
- A. Jézéquel, P. Yiou, and S. Radanovics. Role of circulation in {European} heatwaves using flow analogues. *Climate Dynamics*, 2017a. ISSN 1432-0894. doi: 10.1007/s00382-017-3667-0. URL <https://doi.org/10.1007/s00382-017-3667-0>.
- A. Jézéquel, P. Yiou, S. Radanovics, and R. Vautard. Analysis of the exceptionally warm December 2015 in France using flow analogues. *BAMS*, 2017b.
- E. Kalnay, M. Kanamitsu, R. Kistler, W. Collins, D. Deaven, L. Gandin, M. Iredell, S. Saha, G. White, J. Woollen, Y. Zhu, M. Chelliah, W. Ebisuzaki, W. Higgins, J. Janowiak, K. C. Mo, C. Ropelewski, J. Wang, A. Leetmaa, R. Reynolds, R. Jenne, and D. Joseph. The NCEP/NCAR 40-year reanalysis project, 1996. ISSN 00030007.
- J. E. Kay, C. Deser, A. Phillips, A. Mai, C. Hannay, G. Strand, J. M. Arblaster, S. C. Bates, G. Danabasoglu, J. Edwards, M. Holland, P. Kushner, J.-F. Lamarque, D. Lawrence, K. Lindsay, A. Middleton, E. Munoz, R. Neale, K. Oleson, L. Polvani, and M. Vertenstein. The Community Earth System Model (CESM) Large Ensemble Project: A Community Resource for Studying Climate Change in the Presence of Internal Climate Variability. *Bulletin of the American Meteorological Society*, 96(8):1333–1349, 2015. doi: 10.1175/BAMS-D-13-00255.1. URL <https://doi.org/10.1175/BAMS-D-13-00255.1>.
- G. A. Meehl and C. Tebaldi. More intense, more frequent, and longer lasting heat waves in the 21st century. *Science*, 305(5686):994–997, 2004. URL <Go to ISI>://000223250700045.
- E. P. Meredith, V. A. Semenov, D. Maraun, W. Park, and A. V. Chernokulsky. Crucial role of Black Sea warming in amplifying the 2012 Krymsk precipitation extreme. 8 (August), 2015. doi: 10.1038/NGEO2483.
- J. A. Nelder and R. W. Wedderburn. Generalized Linear Models. *Journal of the Royal Statistical Society Series a-General*, 135(3):370–384, 1972. URL <Go to ISI>://A1972N770800027.
- F. E. L. Otto, N. Massey, G. J. V. Oldenborgh, R. G. Jones, and M. R. Allen. Reconciling two approaches to attribution of the 2010 Russian heat wave. 39(November 2011): 1–5, 2012. doi: 10.1029/2011GL050422.
- F. E. L. Otto, G. J. van Oldenborgh, J. Eden, P. A. Stott, D. J. Karoly, and M. R. Allen. The attribution question. *Nature Climate Change*, 6(9):813–816, 2016. ISSN 1758-678X. doi: 10.1038/nclimate3089. URL <http://www.nature.com/doifinder/10.1038/nclimate3089>.
- H. A. Panofsky and G. W. Brier. *Some applications of statistics to meteorology*. Mineral Industries Extension Services, College of Mineral Industries, Pennsylvania State University, 1958.

- Y. Peings, J. Cattiaux, S. Vavrus, and G. Magnusdottir. Late Twenty-First-Century Changes in the Midlatitude Atmospheric Circulation in the CESM Large Ensemble. *Journal of Climate*, 30(15):5943–5960, 2017. doi: 10.1175/JCLI-D-16-0340.1. URL <https://doi.org/10.1175/JCLI-D-16-0340.1>.
- R. L. Prentice. Binary Regression Using an Extended Beta-Binomial Distribution, with Discussion of Correlation Induced by Covariate Measurement Errors. *Journal of the American Statistical Association*, 81(394):321–327, 1986. doi: 10.1080/01621459.1986.10478275. URL <http://www.tandfonline.com/doi/abs/10.1080/01621459.1986.10478275>.
- S. Rahmstorf and D. Coumou. Increase of extreme events in a warming world. *Proceedings of the National Academy of Sciences of the United States of America*, 108(44):17905–17909, 2011. doi: DOI 10.1073/pnas.1101766108. URL <Go to ISI>://000296373400015.
- S. Russo, A. Dosio, R. G. Graversen, J. Sillmann, H. Carrao, M. B. Dunbar, A. Singleton, P. Montagna, P. Barbola, and J. V. Vogt. Magnitude of extreme heat waves in present climate and their projection in a warming world. *Journal of Geophysical Research: Atmospheres*, 119(22):12,500–512,512, 2014. ISSN 2169-8996. doi: 10.1002/2014JD022098. URL <http://dx.doi.org/10.1002/2014JD022098>.
- S. Russo, J. Sillmann, and E. M. Fischer. Top ten European heatwaves since 1950 and their occurrence in the future. *Environmental Research Letters*, 10(12):124003, 2015. ISSN 1748-9326. doi: 10.1088/1748-9326/10/12/124003. URL <http://dx.doi.org/10.1088/1748-9326/10/12/124003>.
- P. M. Ruti, a. Dell’Aquila, and F. Giorgi. Understanding and attributing the Euro-Russian summer blocking signatures. *Atmospheric Science Letters*, 15(3):204–210, jul 2014. ISSN 1530261X. doi: 10.1002/asl2.490. URL <http://doi.wiley.com/10.1002/asl2.490>.
- S. I. Seneviratne, T. Corti, E. L. Davin, M. Hirschi, E. B. Jaeger, I. Lehner, B. Orlowsky, and A. J. Teuling. Investigating soil moisture-climate interactions in a changing climate: A review. *Earth-Science Reviews*, 99(3-4):125–161, 2010. ISSN 00128252. doi: 10.1016/j.earscirev.2010.02.004. URL <http://dx.doi.org/10.1016/j.earscirev.2010.02.004>.
- S. I. Seneviratne, M. G. Donat, A. J. Pitman, R. Knutti, and R. L. Wilby. Allowable CO₂ emissions based on regional and impact-related climate targets. *Nature*, 529(7587):477–483, 2016. ISSN 0028-0836. doi: 10.1038/nature16542. URL <http://www.nature.com/doifinder/10.1038/nature16542>.
- T. G. Shepherd. A Common Framework for Approaches to Extreme Event Attribution. *Current Climate Change Reports*, 2(1):28–38, 2016. ISSN 2198-6061. doi: 10.1007/s40641-016-0033-y. URL <http://dx.doi.org/10.1007/s40641-016-0033-y>.
- M. Stéfanon, P. Drobinski, F. D’Andrea, and N. De Noblet-Ducoudré. Effects of interactive vegetation phenology on the 2003 summer heat waves. *Journal*

- of Geophysical Research Atmospheres*, 117(24):1–15, 2012. ISSN 01480227. doi: 10.1029/2012JD018187.
- P. A. Stott, D. A. Stone, and M. R. Allen. Human contribution to the European heatwave of 2003. *Nature*, 432(7017):610–614, 2004. doi: Doi 10.1038/Nature03089. URL <Go to ISI>://000225433200043.
- P. A. Stott, N. Christidis, F. E. L. Otto, Y. Sun, J.-P. Vanderlinden, G. J. van Oldenborgh, R. Vautard, H. von Storch, P. Walton, P. Yiou, and F. W. Zwiers. Attribution of extreme weather and climate-related events. *Wiley Interdisciplinary Reviews: Climate Change*, 7(1):23–41, 2016. ISSN 1757-7799. doi: 10.1002/wcc.380. URL <http://dx.doi.org/10.1002/wcc.380>.
- K. E. Taylor, R. J. Stouffer, and G. A. Meehl. An Overview of CMIP5 and the Experiment Design. *Bulletin of the American Meteorological Society*, 93(4):485–498, 2012. doi: 10.1175/BAMS-D-11-00094.1. URL <https://doi.org/10.1175/BAMS-D-11-00094.1>.
- S. Tibaldi and F. Molteni. On the operational predictability of blocking. *Tellus A: Dynamic Meteorology and Oceanography*, 42(3):343–365, 1990. doi: 10.3402/tellusa.v42i3.11882. URL <http://dx.doi.org/10.3402/tellusa.v42i3.11882>.
- K. E. Trenberth and J. T. Fasullo. Climate extremes and climate change: The Russian heat wave and other climate extremes of 2010. 117(July):1–12, 2012. doi: 10.1029/2012JD018020.
- K. E. Trenberth, J. T. Fasullo, and T. G. Shepherd. Attribution of climate extreme events. *Nature Clim. Change*, 5(8):725–730, 2015. ISSN 1758-678X. URL <http://dx.doi.org/10.1038/nclimate2657>.
- R. Vautard, P. Yiou, F. Otto, P. Stott, N. Christidis, G. J. van Oldenborgh, and N. Schaller. Attribution of human-induced dynamical and thermodynamical contributions in extreme weather events. *Environmental Research Letters*, 11(11): 114009, 2016. URL <http://stacks.iop.org/1748-9326/11/i=11/a=114009>.
- E. T. Whittaker and G. N. Watson. *A course of modern analysis*. Cambridge university press, 1996.
- T. W. Yee. *Journal of Statistical Software*. 32(10), 2010. doi: 10.18637/jss.v032.i10.
- P. Yiou and M. Nogaj. Extreme climatic events and weather regimes over the North Atlantic: When and where? *Geophysical Research Letters*, 31:1–4, 2004. doi: 10.1029/2003GL019119.
- P. Yiou, A. Jézéquel, P. Naveau, F. E. L. Otto, R. Vautard, and M. Vrac. A statistical framework for conditional extreme event attribution. *Advances in Statistical Climatology, Meteorology and Oceanography*, 3(1):17–31, 2017. doi: 10.5194/ascmo-3-17-2017. URL <http://www.adv-stat-clim-meteorol-oceanogr.net/3/17/2017/>.
- G. Zappa and T. G. Shepherd. Storylines of atmospheric circulation change for European regional climate impact assessment. *Journal of Climate*, 30(16):6561–6577, 2017. ISSN 08948755. doi: 10.1175/JCLI-D-16-0807.1.